Experimental investigation on the flexural behaviour of stainless steel reinforced concrete beams

Musab Rabi[a], Rabee Shamass[b], K.A. Cashell[c]

[a] Dept of Civil Engineering, Jerash University, Jordan, Musab.rabi@jpu.edu.jo

[b] Division of Civil and Building Services Engineering, School of the Built Environment and Architecture, London South Bank University, UK

[c] Dept of Civil and Environmental Engineering, Brunel University London, UK

Abstract

The durability of reinforced concrete (RC) structures and infrastructure has been the subject of significant attention from the engineering research community in recent years, mainly owing to the deterioration of RC elements due to corrosion of the embedded steel reinforcement. In this context, stainless steel reinforcement can provide an efficient solution to enhance the expected lifetime of concrete structures, reducing the damage due to corrosion of the reinforcement and carbonation and deterioration of the concrete. However, current international design standards for reinforced concrete structures do not include appropriate guidance for stainless steel reinforced concrete (SSRC). In order to investigate the behaviour of stainless steel RC beams, a series of six beam tests was conducted and is discussed herein. The key performance measures for RC beams such as load-deflection response, cracking behaviour and deflections at service load are assessed. The validity and applicability of existing design rules, which were developed for carbon steel RC, are also examined for stainless steel reinforced concrete members. Other recently developed design procedures, based on the Continuous Strength Method and including an accurate material model for the stainless steel bars, are also examined.

Keywords: Stainless steel reinforcement; Reinforced concrete beams; Continuous strength method, Experimental tests; Deflections; Design guidance; Deflections, Serviceability.

1. Introduction

The use of stainless steel in structural applications has been steadily increasing in recent years primarily due to its distinctive and attractive physical and mechanical properties, as well as the availability of efficient and user-friendly design guidance. Stainless steel is known for its corrosion resistance and also offers excellent mechanical properties, very good fire resistance, a long life cycle compared with carbon steel, is

fully recyclable at the end of its service life, and has low maintenance requirements (Rabi et al., 2022; Gedge, 2003). These advantageous characteristics are dependent on the constituent elements of the stainless steel alloy in question, as well as the production route, finish and product form. From a structural perspective, the key properties of stainless steel which distinguish it from other structural materials are its nonlinear constitutive response, its good weldability and excellent mechanical characteristics including exceptional ductility.

Stainless steels are defined as a group of metals containing a minimum chromium content of 10.5% and a maximum carbon content of 1.2% (EN 10088-1, 1995). The chromium improves the corrosion resistance of stainless steel through the development of a passive protective layer on the surface in the presence of oxygen (Evans, 2002). There are five main categories of stainless steel, according to their metallurgical structure, including the austenitic, duplex, ferritic, martensitic and precipitation hardened grades. The austenitic and duplex grades are most commonly used in structural applications owing to the exceptional corrosion resistance and outstanding mechanical properties (Baddoo and Burgan, 2012; Gardner, 2005). In addition, the ferritic grades are increasingly attractive in appropriate structural applications that do not require high corrosion resistance material (Baddoo, 2008).

To date, the most common use of stainless steel in load-bearing applications is as bare structural sections such as for columns and beams. In more recent years, stainless steel has emerged as a useful material for reinforcement in concrete structures. Although it has generally been limited to very specific scenarios (e.g. splash zones in bridges, harsh environments), this is changing as the attributes of stainless steel as a durable material are more recognised and attractive, and previously-lacking performance data is becoming more available.

Reinforced concrete (RC) is an efficient and economical structural solution, but corrosion of the reinforcement is a fundamental challenge, particularly in industrial, marine and polluted environments. The typical measures used to improve the durability of RC structures such as using sealants or membranes on the concrete surface, increasing the concrete cover and employing cement inhibitors (British Stainless Steel Association, 2003) may not prevent the development of unacceptable levels of corrosion and do not provide an environmentally-sustainable solution. In this context, there are growing demands to improve the durability and service life of reinforced concrete structures, especially for key infrastructure such as bridges and tunnels. Stainless steel RC can offer an ideal and efficient solution, extending the lifetime of the structure, reducing the economic and embodied carbon costs, and minimising expensive inspection, maintenance and monitoring expenses (Val and Stewart, 2003). Although stainless steel reinforcement has a relatively higher initial cost compared to traditional carbon steel, the use of stainless steel reinforcement can reduce the overall maintenance costs by up to 50% (Cramer et al., 2002).

As stated before, stainless steel exhibits a quite different constitutive response compared with carbon steel, as it is highly non-linear even at low strains and develops significant levels of strain hardening and ductility, as shown in Figure 1. However, current design standards such as Eurocode 2 (2004) and ACI 318-11 (2011) do not provide realistic constitutive material models for stainless steel reinforcement, and instead include simplistic elastic-plastic idealisations, which are not representative of the real behaviour. It has been shown that using the carbon steel RC design equations to estimate the flexural performance of stainless steel RC members results in overly-conservative capacity predictions (Rabi et al., 2019a). Therefore, this approach is neither efficient nor realistic.

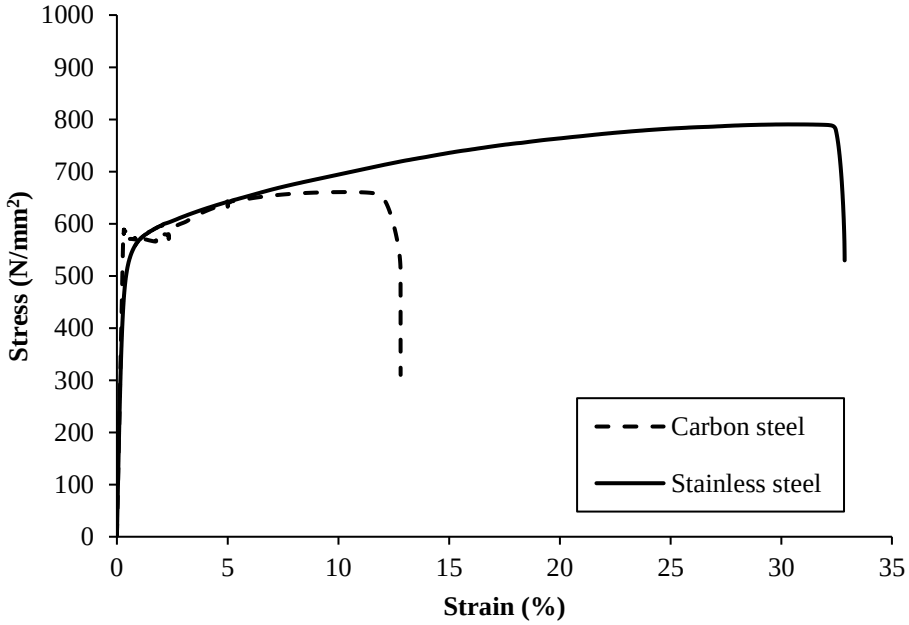

Figure 1: Stress-strain constitutive response for stainless steel grade 1.4301 and carbon steel, with diameter of 10 mm (Rabi et al., 2020).

There has been some research in recent years into stainless steel reinforcement, mainly focussed on the corrosion behaviour (Alonso et al., 2019; Fahim et al., 2019; Lollini et al., 2018; Serdar et al., 2013; Alvarez et al., 2011) as well as limited studies into the bond behaviour (Rabi et al., 2020; Aldaca et al., 2018; Zhou et al., 2017). Research into the response of structural members has been more limited and there is a lack of experimental data on the flexural behaviour of stainless steel RC beams (Rabi et al., 2022). Alih and Khelil (2012) tested a single stainless steel RC beam but did not reach the ultimate load capacity of the beam. Medina et al. (2015) also reported two tests on short beams (1 m in length) reinforced with stainless steel rebars. These resulted in brittle failures, and the influence of the distinctive strain hardening and ductility properties of stainless steel were not fully explored. In addition, a new design model was recently proposed

which harnesses the advantageous strain hardening and ductility of stainless steel into the design of reinforced concrete members (Rabi et al., 2019a). In light of the absence of performance data on stainless steel reinforced concrete beams, the current paper aims to experimentally investigate the flexural behaviour of these members, examining the influence of different parameters such as reinforcement ratio and stainless steel grade. The accuracy of existing design codes and the method proposed by Rabi et al. (2019a) is also investigated. The paper proceeds with an overview of this method, followed by a detailed discussion on the experimental programme.

2. Flexural design of stainless steel reinforced concrete members using the CSM

The continuous strength method (CSM) is a deformation-based design procedure which accounts for material nonlinearity and enables strain hardening to be exploited in the capacity calculations, resulting in more efficient and accurate results. This method predicts the cross-sectional resistance of the member depending on two main components: (1) a base curve that defines the relationship between the limiting strain at the ultimate load and the cross-section slenderness, and (2) a material model that allows for strain hardening. The CSM was originally developed for bare stainless steel non-slender cross-sections (Gardner and Nethercot, 2004), and has since been expanded to include the design of structural steel members (Gardner et al., 2011; Afshan and Gardner, 2013), composite elements (Gardner et al., 2017; Shamass and Cashell, 2018) and stainless steel reinforced concrete beams (Rabi et al., 2019a, 2019b, 2021). With reference to the latter, a similar approach is adopted to develop a deformation-based design method for reinforced concrete beams with stainless steel rebar, accounting for the true stainless steel constitutive relationship. Two different versions of the method were developed comprising a full and simplified design approach. The full analytical model employs the modified Ramberg-Osgood material model (Mirambell and Real, 2000; Rasmussen, 2003) to represent the nonlinear behaviour of stainless steel whilst the simplified model adopts a bi-linear stress-strain relationship; both are presented in Figure 2. The modified Ramberg-Osgood material model is an extension of the original expression proposed by Ramberg and Osgood (1943) in which the stress-strain response are obtained using Equations (1 and 2) for the elastic and non-elastic stages of the behaviour, respectively:

$$\varepsilon = \frac{\sigma}{E} + 0.002\left(\frac{\sigma}{\sigma_{0.2}}\right)^{n} \quad \text{for} \quad \sigma \leq \sigma_{0.2} \tag{1}$$

$$\varepsilon = \varepsilon_{0.2} + \frac{\sigma-\sigma_{0.2}}{E_2} + \left(\varepsilon_u - \varepsilon_{0.2} - \frac{\sigma_u-\sigma_{0.2}}{E_2}\right)\left(\frac{\sigma-\sigma_{0.2}}{\sigma_u-\sigma_{0.2}}\right)^{m} \quad \text{for} \quad \sigma_{0.2} < \sigma \leq \sigma_u \tag{2}$$

In these expressions, σ and ε are the engineering stress and strain, respectively, σ_u and ε_u are the ultimate stress and corresponding ultimate strain, respectively, $\sigma_{0.2}$ and $\varepsilon_{0.2}$ are the 0.2% proof stress, which is

typically used to identify the yield limit in stainless steel, and the corresponding strain, respectively, E is the elastic modulus, E_2 is the tangent modulus at $\sigma_{0.2}$, and n and m are strain hardening material constants. It is noteworthy that all equations in this paper are applied using SI units, unless it is explicitly stated otherwise. The bi-linear material model employed in the simplified analytical model, as shown in Figure 2, is obtained using the expressions given in Equations (3 and 4):

$$\sigma = E\varepsilon \qquad \varepsilon \leq \varepsilon_y \tag{3}$$

$$\sigma = \sigma_{0.2} + E_{sh}(\varepsilon - \varepsilon_y) \qquad \varepsilon > \varepsilon_y \tag{4}$$

This approach defines the yield point as the 0.2% proof stress ($\sigma_{0.2}$) and the corresponding yield strain (ε_y) as the ratio between $\sigma_{0.2}$ and the elastic modulus E. The difference between ε_y and $\varepsilon_{0.2}$ as employed in the full material model is demonstrated in Figure 2. The modulus of elasticity for the strain hardening region E_{sh} is obtained as the slope of the line crossing the yield (ε_y, $\sigma_{0.2}$) and ultimate ($C_2\varepsilon_u$, σ_u) points, as given in Equation (5). It has been shown that a C_2 value of 0.25 is appropriate for reinforced concrete beams with austenitic stainless steel grades 1.4311 and 1.4307, whereas a value of 0.3 is more suitable for beams with lean duplex stainless steel grade 1.4162 (Rabi et al., 2019a).

$$E_{sh} = \frac{\sigma_u - \sigma_{0.2}}{C_2\varepsilon_u - \varepsilon_y} \tag{5}$$

The full and simplified design models employ the equations of equilibrium to the cross-section, together with the material models, to obtain the plastic bending moment capacity of stainless steel reinforced concrete beams. The internal forces are determined based on the stainless steel stress-strain material model and the equivalent rectangular compressive stress distribution in the concrete, together with the strain distribution in the section. The stress in the reinforcement at failure is determined based on the assumed failure strain and the strain distribution in the section. More detailed descriptions of the full and simplified models are available elsewhere (Rabi et al., 2019a).

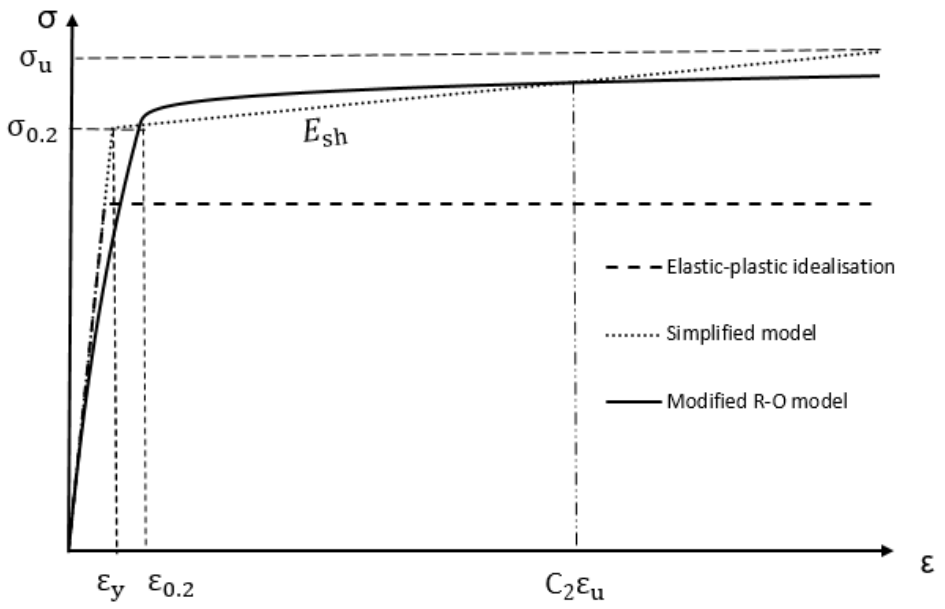

Figure 2: The modified Ramberg-Osgood material model and the simplified version for stainless steel.

3. Experimental programme

An experimental series comprising six stainless steel reinforced concrete beams were cast and tested in the structural engineering laboratory at London South Bank University. A further beam reinforced with carbon steel rebars was also examined, for comparison. The aim of the study was to investigate the flexural behaviour and load-carrying capacity of these members. Two different grades of austenitic stainless steel (1.4301 and 1.4436) and three different reinforcement ratios (0.46%, 0.72% and 1.04%) were considered. The mechanical properties of the reinforcement was obtained using standard tension tests of rebars, in according to (EN 6892-1, 2016) while the concrete material characteristics were obtained using standard compression tests, as discussed hereafter.

3.1. Material properties

3.1.1. Concrete

The mix proportions designed to produce a target concrete compressive strength of C30/37 are 0.54 water-to-cement ratio, 463 kg/m^3 ordinary cement and 700 kg/m^3 and 927 kg/m^3 sand and course aggregate, respectively. The max aggregate size used was 10 mm. In addition to the beam specimens, five 100×100 mm cubes were cast from the same batch to enable compressive material strength tests to be conducted on the day of beam testing, in accordance with the guidance given in (EN 12390-3, 2009). After casting, the beams and cubes were covered with wet burlap and plastic sheets and cured at room temperature. The average concrete compressive strength f_c for each beam is given in Table 2, taken as the average from 5 cube tests conducted on the day of beam testing.

3.1.2. Stainless steel reinforcement

Austenitic stainless steels are the most common grades used for reinforcement owing to their excellent mechanical properties and outstanding corrosion resistance (Gardner et al., 2016). In the current study, austenitic stainless steel grades 1.4301 (AISI 304) and 1.4436 (AISI 316) were selected as these are commonly available from local suppliers. Three different stainless steel bar diameters were considered including 8 mm, 10 mm and 12 mm rebars. All of the stainless steel reinforcement comprised two series of transverse ribs at each cross-section, whilst the carbon steel bars had two longitudinal ribs as well as two transverse ribs at each cross-section. The stainless steel and carbon steel reinforcement complied with the requirements provided in (BS 6744, 2016) and (BS 4449, 2005), respectively.

The chemical compositions of the stainless steel reinforcement, according to the product certificate provided by the manufacturer, are presented in Table 1. The mechanical properties of the stainless steel reinforcement was determined by conducting tensile tests, to obtain the stress-strain constitutive response. These were conducted in accordance with (EN 6892-1, 2016), and the results are given in Table 2 and Figure 3. Three repeat tests were carried out on each type of bar, and the average response is taken for the value presented. Table 2 also includes the material data for the tests reported by Li et al. (2020), which are used later in this paper for further validation and analysis. In this table, σ_y is the yield strength of the rebar (which is taken as the 0.2% proof strength $\sigma_{0.2}$ for stainless steel), σ_u is the ultimate strength of the reinforcement, ε_u is the elongation at failure of the reinforcement and δ_u is the mid-span deflection corresponding to the ultimate load capacity P_u. The tension reinforcement arrangement for each beam is described in the table by the number and diameter of the rebars (e.g. 2Ø8 refers to 2 bars with a diameter of 8 mm). The results presented in Figure 3 show the stress-strain material response for stainless and carbon steel reinforcing bars with different bar diameters. It is clear that the stainless steel samples exhibited nonlinear behaviour from an early stage followed by a continuous, rounded response with significant strain hardening and ductility.

Table 1: Stainless steels chemical composition

Stainless steel grade	**% C**	**% Mn**	**% Si**	**%S**	**% P**	**% Ni**	**% Cr**	**% Mo**	**% N**
1.4436	0.014	1.44	0.39	0.002	0.038	10.60	16.75	2.60	0.0770
1.4301	0.032	1.72	0.46	0.004	0.039	8.10	18.40	0.24	0.1830

Table 2: Material properties and beam test results

Beam	**f_c (N/mm^2)**	**Grade**	**Tension reinforcement**	**σ_y (N/mm^2)**	**σ_u (N/mm^2)**	**ε_u%**	**E (kN/mm^2)**	**P_u (kN)**	**δ_u (mm)**
Tests in current test programme									

SS43-D8	32.3	1.4301	2Ø8	720	888	44.6	156	44.0	21.48
SS44-D8	32.3	1.4436	2Ø8	614	823	36.5	178.5	39.5	20.62
SS43-D10	32.3	1.4301	2Ø10	668	799	38.3	148.6	55.7	23.47
SS44-D10	32.3	1.4436	2Ø10	661	793	25.6	179.3	60.2	25.62
SS43-D12	41.7	1.4301	2Ø12	670	795	26.7	186.8	88.4	24.96
SS44-D12	42.4	1.4436	2Ø12	645	803	25.3	198.6	78.6	23.63
CS-D10	32.3	B500B	2Ø10	525	627	20.1	196	48.7	8.80
Beams tested by Li et al. (2020)									
BKW1	41.9	1.4462	2Ø12	660	830	38	141	145	23.9
BKW2	41.5	1.4462	2Ø12	660	830	38	141	145	25.9
PKW1	40.1	HRB335	2Ø12	380	530	31	230	100	7.93

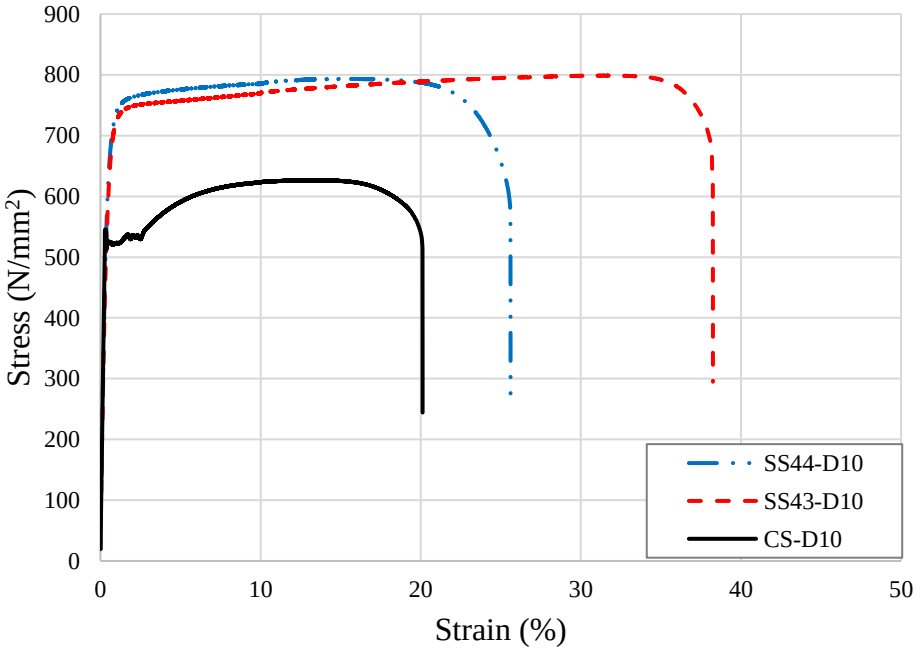

(a)

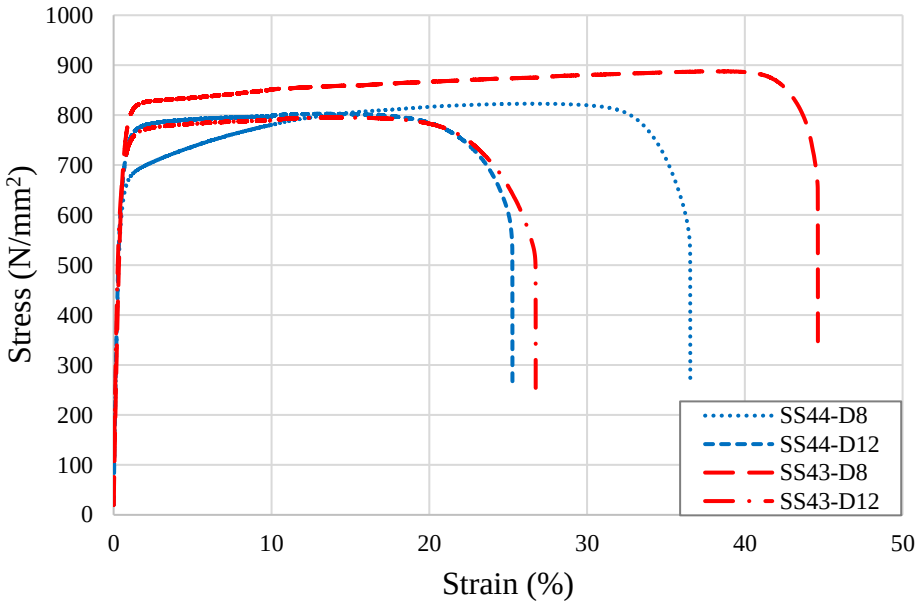

(b)

Figure 3: Stress-strain behaviour for stainless steel and carbon steel reinforcement with a diameter of (a) 10 mm and (b) 8 and 12 mm.

3.2. Beam tests

A total of seven beam tests were conducted, as shown in Table 2, comprising six with stainless steel reinforcement and one with carbon steel rebar, for comparison. Three of the beams were reinforced with grade 1.4301 stainless steel (specimens SS43-D8, SS43-D10 and SS43-D12), three contained grade 1.4436 stainless steel (SS44-D8, SS44-D10 and SS44-D12) and the final beam had carbon steel B500B reinforcement (CS-D10). A reference-system was adopted to define each specimen, in which the first term denotes the reinforcement type and grade (i.e. SS43 is stainless steel grade 1.4301, SS44 is stainless steel grade 1.4426 and CS is carbon steel), and the second term defines the rebar diameter (D8, D10 and D12 for bars with a diameter of 8 mm, 10 mm and 12 mm, respectively). Figure 4 presents (a) a schematic elevation view of the beams configuration including the reinforcement and geometrical details and (b) a photograph showing the moulds used to arrange the reinforcement before and after concrete casting.

All of the beams had a height h of 200 mm, a width b of 125 mm and an overall length L of 2000 mm. The beams were tested under four-point loading conditions over a clear span L of 1800 mm. The length of the constant moment zone in the middle of the beam was 500 mm and the thickness of the clear concrete cover was 23 mm at the sides of the beam and 20 mm at the top and bottom of the beam, measured from the surface of the longitudinal reinforcement to the outer surface of the concrete. The tensile reinforcement

in the lower region of the beam was either stainless steel or carbon steel with bar diameter of 8 mm, 10 mm and 12 mm whilst the top reinforcement in the compression region and shear stirrups were made from carbon steel and had a diameter of 8 mm. In all beams, shear stirrups were included at intervals of 100 mm in the shear region to avoid the shear failure.

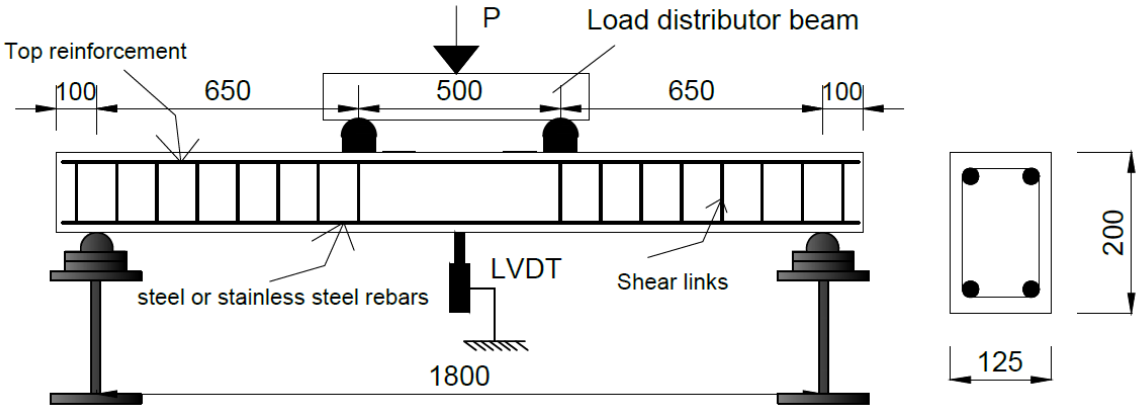

(a)

(b)

Figure 4: Beam specimen configuration including (a) the reinforcement and geometrical details (all dimensions in mm) and (b) moulds ahead of casting, showing the reinforcement arrangement

In order to provide a more robust discussion on the behaviour, the test results from another experimental programme on both carbon steel and stainless steel RC beams are also discussed in the current paper (Li et al., 2020). This programme included three simply-supported beams which were 2400 mm in length,

examined under four-point loading, and reinforced with either grade 1.4462 stainless steel (2 specimens) or grade HRB335 carbon steel (1 specimen). The results from these tests are presented in Table 2 and more detail is presented later, where relevant to the discussion.

3.3. Instrumentation and testing procedure

A hydraulic testing machine with a capacity of 250 kN was used to apply a monotonic concentrated load on a load distributer beam, which delivered two equal point loads to the top surface of the beam (Figure 5). The load was applied in displacement-control at a rate of 1 mm/min in all tests. The vertical deflection at the middle of the span was measured and recorded using linear variable differential transducers (LVDTs). An automatic-data acquisition system connected to a computer was used to monitor loading and deflections during the test. Prior to testing, all of the specimens were painted white as shown in Figure 5 so that the development of cracks and crack patterns could be readily observed. During the tests, once the first crack was visible, loading was paused and the location and size of the crack was marked on the beam. The tests were then re-started and the cracks were marked at 10 kN intervals.

Figure 5: An image of a beam being tested under four point loading.

4. Test results and discussion

In this section, the main findings and observations from the tests are discussed and analysed. The key performance measures for reinforced concrete beams are assessed, including the load-deflection responses, ultimate moment capacities, cracking moments, crack patterns, and deflections at service load. Comparisons are also made with the capacities obtained from Eurocode 2 (2004) and ACI 318-11 (2011). The predicted ultimate moment capacity obtained using the CSM design procedure, as discussed before, is also compared with the experimental values.

4.1. Load-deflection response

The load-deflection responses for all seven examined beams are presented in Figure 6. In addition, the ultimate load P_u and corresponding deflection δ_u are given in Table 2. In general, all beams performed well

during the tests, demonstrating good ductility and sufficient warning of failure. At low load levels, all of the beams behaved similarly, in terms of the initial stiffness and the first cracking point. Soon after the cracking moment was reached however, the stainless steel RC beams exhibited a more nonlinear and rounded response compared with CS-D10. With reference to the data in Figure 6 and Table 2, some more detailed, key observations from the load-deflection responses are as follows:

- The beams with greater reinforcement ratios (i.e. SS43-D12 and SS44-D12) reached greater ultimate loads P_u, as expected, compared with the other beams. Following the attainment of the peak load, the capacity of the stainless steel reinforced concrete beams reduced gradually until failure occurred by crushing of the concrete, thus resulting in a ductile failure. The behaviour depended on the reinforcement ratio and the grade of the stainless steel. For instance, beam SS44-D10 had a stiffer response compared with SS44-D8.
- Beam CS-D10 with carbon steel rebars had a more linear response compared with the stainless steel RC beams until its peak load of around 44 kN was reached. This was followed by a short yield plateau and slight increase in the loading capacity due to strain hardening in the steel rebar. Failure occurred by yielding of the reinforcement.
- As expected, the beams with greater reinforcement ratios reached greater peak loads. However, it is interesting to note that the ductility and deflection at ultimate load were greater for the beams with lower reinforcement ratios. This is most likely because as the reinforcement ratio increased, the levels of stress and strain in the rebars reduced and hence, strain hardening in the stainless steel rebars was not fully exploited and the behaviour became less ductile.
- Specimens CS-D10, SS43-D10 and SS44-D10 had the same reinforcement ratio, geometry and concrete strength, but had different reinforcing material. CS-D10 demonstrated a stiffer initial response compared with the stainless steel RC beams, but yielded sooner and had a less ductile response overall. However, the deflection δ_u at the ultimate load was almost three times greater for the stainless steel RC specimens, compared with CS-D10, as given in Table 2. There are likely to be a number of contributing factors to this, including the likely lower bond strength which exists between stainless steel reinforcement and concrete compared with carbon steel rebars and the surrounding concrete, as concluded in Rabi et al. (2020). This leads to greater distribution of strains in the rebar, and more cracking throughout the member, resulting in higher levels of ductility and deflection. In addition, P_u was almost 20% greater for the stainless steel RC beams. This is owing to the different constitutive relationships of the two materials, as previously discussed. Carbon steel has a linear elastic stress-strain response until yielding occurs, followed by a yield plateau and then

limited strain hardening until failure. On the other hand, stainless steel has a more nonlinear stress-strain response, with no clearly-defined yield point, and excellent ductility, as shown in Figure 3.

- In terms of the failure mode, all of the stainless steel RC beams failed in a ductile manner, by crushing of the concrete, whilst the carbon steel RC beam failed by yielding of reinforcement. This is owing to the significant strain hardening and ductility of the stainless steel rebars, compared with the carbon steel reinforcement, and resulted in the stainless steel RC beams exhibiting sufficient warning before collapse occurred, including reaching large levels of deflection accompanied by significant cracking , as shown in Figures 6, 7 and 8, respectively.

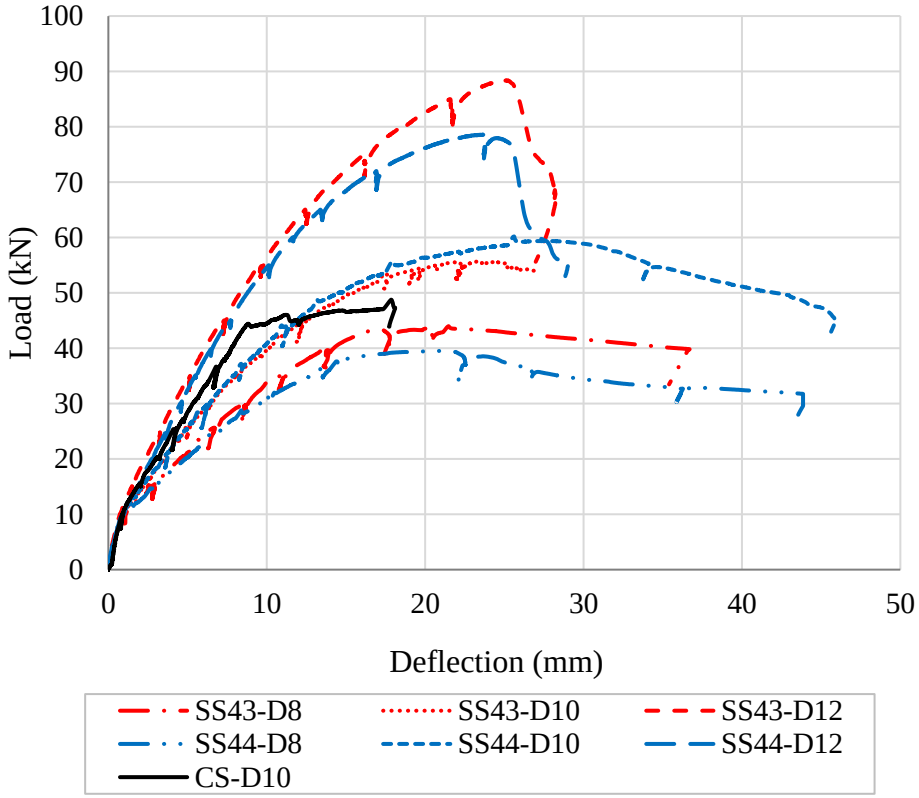

Figure 6: Load-mid span deflection curves for stainless steel beams in comparison with carbon steel beam.

4.2. Ultimate bending capacity

The experimental ultimate bending moment values for each of the test specimens ($M_{u,EXP}$) are presented in Table 3 together with the corresponding design values ($M_{u,des}$) from Eurocode 2 (2004) and ACI 318-11 (2011). The test data from Li et al. (2020), as previously described, are also presented. In addition, Table 3 includes the design capacities predicted using the full CSM approach previously described ($M_{u,FCSM}$) as well as the simplified version $M_{u,SCSM}$. The ratios of the design values (for the codes and the CSM) to the experimental values are also given, for comparison.

It is observed that the ultimate moment capacity of the beams reinforced with stainless steel grade 1.4301 was around 5% greater, on average, than the corresponding values for beams reinforced with grade 1.4436 stainless steel. This is mainly because grade 1.4301 has higher proof and ultimate strength compared to grade 1.4436. The results also show that the bending moment capacity for beams SS44-D10 and SS43-D10 were 23.5% and 14.4% higher than the corresponding value for CS-D10, respectively. This is mainly attributed to the significant strain hardening and greater ductility in the stainless steel reinforcement which enabled SS44-D10 and SS43-D10 to achieve greater moment capacities even after reaching their proof strength values.

The ultimate moment capacity for singly reinforced concrete members in accordance with Eurocode 2 $M_{u,EC2}$ and ACI 318-11 $M_{u,ACI}$ is determined by applying equilibrium of the internal forces and adopting an equivalent rectangular stress distribution through the section, together with an elastic-perfectly plastic constitutive material model of the reinforcement. Thus, $M_{u,EC2}$ and $M_{u,ACI}$ are determined using the Equations (6 and 7), respectively:

$$M_{u,EC2} = f_y A_s \left(d - \frac{\lambda x}{2}\right) \tag{6}$$

$$M_{u,ACI} = \rho f_y b d^2 \left(1 - 0.59 \frac{\rho f_y}{f_c}\right) \tag{7}$$

In these expressions, A_s is the cross-sectional area of steel reinforcement, d is the effective depth from the top of a reinforced concrete beam to the centroid of the tensile reinforcement, ρ is the tensile reinforcement ratio, f_c is the compressive strength of the concrete and b is the width of the cross-section. λx is determined in accordance with Equation (8):

$$\lambda x = \frac{A_s f_y}{\eta\, \alpha_{cc} f_c b} \tag{8}$$

where η is taken as 1 for $f_c \leq 50$ MPa, in accordance with Eurocode 2, and α_{cc} is taken as 0.85 as recommended by the UK National Annex to Eurocode 2 (2009). In the current specimens, both codes give identical predictions of the ultimate moment capacity (i.e. $M_{u,EC2} = M_{u,ACI} = M_{u,des}$) as they are based on the same beam bending theory and adopt equivalent reinforcement material models. With reference to the values given in Table 3, the design codes are shown to provide a conservative estimation of the ultimate moment capacity for all of the examined beams with the average ratio of design to experimental ultimate moments being 0.85 for the stainless steel RC beams and 0.78 for the carbon steel RC beam. The flexural capacity predictions are somewhat less conservative for the stainless steel RC beams compared with the

carbon steel reinforced members. This is expected given the higher proof strength of the stainless steel reinforcement compared with carbon steel rebars, as indicated in Table 2.

Additionally, there is an excellent agreement between the experimental values and those obtained analytically using the full and simplified CSM with an average ratio of the capacity prediction to the corresponding experimental value for all beams of 0.89 (full CSM) and 0.87 (simplified CSM), respectively. Clearly, the full and simplified continuous strength methods provide consistently conservative predictions of the ultimate bending moment capacity but are more accurate and realistic than those predicted by the international design standards. It is also noteworthy that the simplified CSM approach, which is straight-forward to apply using only information which is readily available to designers, provides very good results compared with the existing design codes.

Table 3: Comparison of the experimental and design ultimate bending moments for the test beams

Specimen	**$M_{u,EXP}$ (kNm)**	**$M_{u,des}$ (kNm)**	**$M_{u,des}/M_{u,Exp}$**	**$M_{u,FCSM}$ (kNm)**	**$M_{u,FCSM}/M_{u,Exp}$**	**$M_{u,SCSM}$ (kNm)**	**$M_{u,SCSM}/M_{u,Exp}$**
SS43-D8	14.30	11.71	0.82	12.58	0.88	12.27	0.86
SS44-D8	12.84	10.11	0.79	11.21	0.87	10.80	0.84
SS43-D10	18.12	16.35	0.90	16.99	0.94	16.70	0.92
SS44-D10	19.56	16.20	0.83	17.00	0.87	16.60	0.85
SS43-D12	28.72	23.27	0.81	22.22	0.77	22.50	0.78
SS44-D12	25.55	22.57	0.88	21.92	0.86	21.88	0.86
CS-D10	15.84	13.19	0.83	-	-	-	-
BKW1	44.63	38.45	0.86	42.68	0.96	40.91	0.92
BKW2	44.63	38.42	0.86	42.63	0.96	40.85	0.92
PKW1	31.13	22.73	0.73	-	-	-	-
Average for SS			0.85	-	0.89	-	0.87
COV for SS (%)			4.64	-	6.9	-	5.5
Average for CS			0.78	-	-	-	-
COV for CS (%)			9.27	-	-	-	-

4.3. Cracking behaviour

For reinforced concrete beams, the development and propagation of cracks is very influential to both the overall and failure behaviour, as well as the ductility and development of stress concentrations. It is

affected by many inter-related parameters such as concrete strength, bond, reinforcement ratio and reinforcement type. Accordingly, during the test programme, considerable attention was given to monitoring the development of cracks, including measurement of the first cracking moment and the development of crack patterns; both are discussed in the current section.

The bending moments corresponding to the first visible crack $M_{cr,EXP}$ were recorded during the experiments and the results are given in Table 4. These are compared with the theoretical cracking moment, calculated as follows:

$$M_{cr} = \frac{f_r I_g}{y_t} \quad (9)$$

where f_r is the modulus of rupture of the concrete, I_g is the gross second moment of area of the section and y_t is the vertical distance between the neutral axis and the outer tension surface of the beam. Eurocode 2 Part 1-1 (2004) and ACI 318-11 (2011) include expressions for f_r, as given in Equations (10 and 11), respectively, which are used together with Equation (9) to determine $M_{cr,EC2}$ and $M_{cr,ACI}$, respectively; the calculated values are included in Table 4:

$$f_{r,EC2} = 0.3(f_c)^{2/3} \quad (10)$$

$$f_{r,ACI} = 0.62\sqrt{f_c} \quad (11)$$

Table 4: Experimental and design cracking moments for the test beams

Specimen	**$M_{cr,EXP}$ (kNm)**	**$M_{cr,EXP}$/ $M_{u,EXP}$**	**$M_{cr,EC2}$ (kNm)**	**$M_{cr,EC2}$/ $M_{cr,Exp}$**	**$M_{cr,ACI}$ (kNm)**	**$M_{cr,ACI}$/ $M_{cr,Exp}$**
SS43-D8	3.3	0.23	2.19	0.66	2.63	0.80
SS44-D8	3.48	0.27	2.19	0.63	2.63	0.75
SS43-D10	3.30	0.18	2.19	0.66	2.63	0.8
SS44-D10	3.25	0.17	2.19	0.67	2.63	0.81
SS43-D12	3.25	0.11	2.59	0.8	2.98	0.92
SS44-D12	2.86	0.11	2.62	0.92	3.01	1.05
CS-D10	3.28	0.21	2.19	0.67	2.63	0.8
BKW1	10.43	0.23	7.02	0.67	8.08	0.77
BKW2	10.88	0.24	6.98	0.64	8.04	0.74
PKW1	11.33	0.36	6.82	0.60	7.90	0.70

Average for SS	0.19	-	0.71	-	0.83
COV for SS (%)	31.1	-	14.0	-	12.6
Average for CS	0.29	-	0.63	-	0.75
COV for CS (%)	38.9	-	7.2	-	9.7

As expected, the experimental cracking moments for beams SS4-D10, SS43-D10 and CS-D10 were very similar as this term is largely dictated by the concrete strength. The data in Table 4 shows that both the European and American design codes provide conservative first-cracking moment predictions, with the ACI code being relatively less conservative. The average ratio of the design cracking moment to the corresponding experimental value for the stainless steel RC beams in this programme was 0.72 for Eurocode 2 and 0.85 for ACI 318-11. The corresponding values for the carbon steel beam were 0.67 and 0.80, respectively. Similar conclusions were found when comparing the tests results from Li et al. (2020) with the design code predictions, as presented in Table 4, where the average predicted-to-experimental cracking moments from Eurocode 2 and ACI 318-11 were 0.66 and 0.76 for the stainless steel RC beams and 0.6 and 0.7 for carbon steel RC beam, respectively.

Figures 7 and 8 present a series of images from two of the tests, namely SS44-D10 and CS-D10, respectively, illustrating the development of cracks as the applied load was increased to the ultimate value. These beams are presented herein for illustrative purposes and comparable behaviour was observed for all of the other beams in this study. For both of these beams, a large number of cracks developed in the constant-moment region. These cracks tended to propagate vertically upwards towards the compression zone. As the load level increased, a few new cracks formed in the shear region (i.e. the region between the support and the application of the point load) and these tended to propagate diagonally towards the location of load application, owing to the combination of flexural and shear stresses in this zone. The other important observation from these images is related to the failure mode. As stated before, it was observed that the stainless steel RC beam failed by crushing of the concrete whereas the beam reinforced with traditional carbon steel rebars failed by yielding of the reinforcement. This is due mainly to the high levels of ductility in the stainless steel reinforcement, compared with the carbon steel rebar. This ductility together with the re-distribution of strains in the rebar at high levels of deflection, enabled a ductile failure behaviour which was characterised by a gradual reduction in the load bearing capacity of the beam after the peak load (as shown in Figure 6).

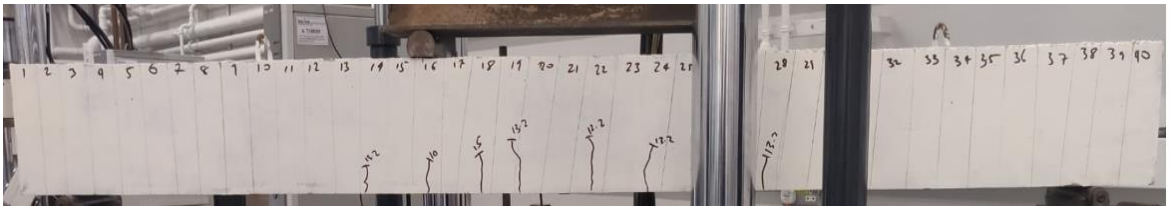

(a)

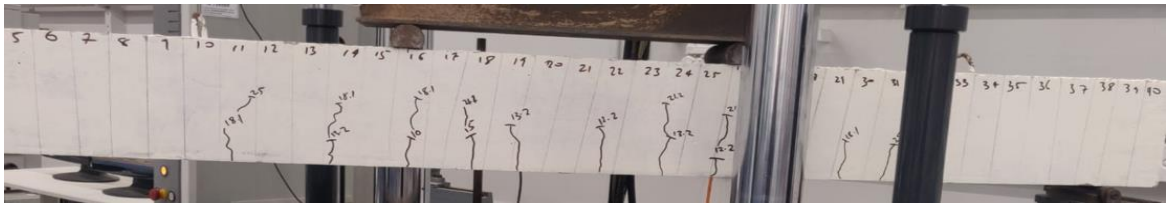

(b)

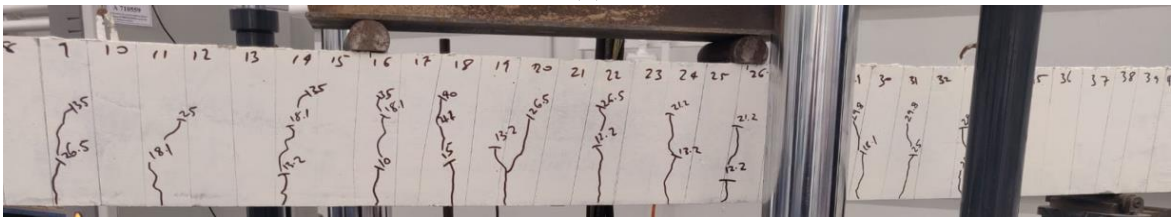

(c)

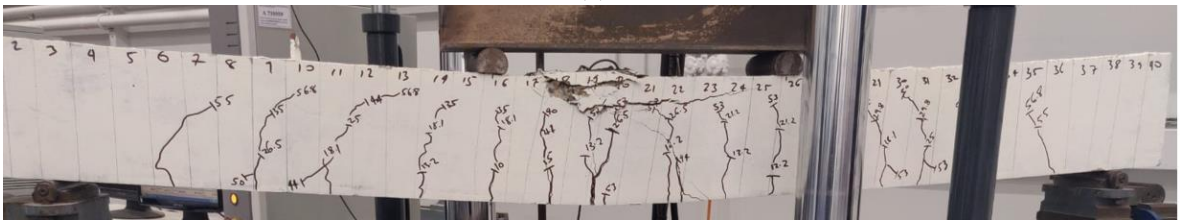

(d)

Figure 7: Development and propagation of crack patterns for stainless steel RC beam SS44-D10 at different levels of applied load, including (a) P=13.2 kN, (b) P=25 kN, (c) P=40 kN, and (d) $P=P_u$=60.2 kN.

(a)

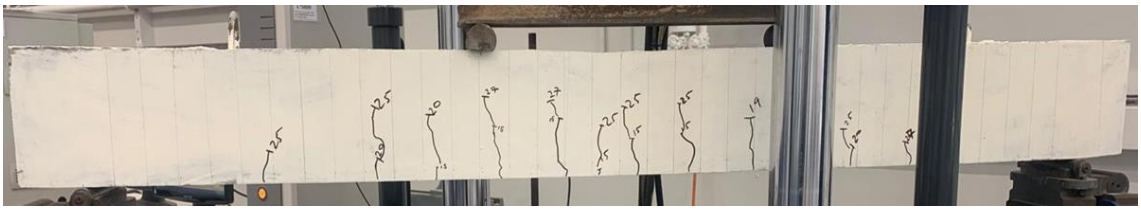

(b)

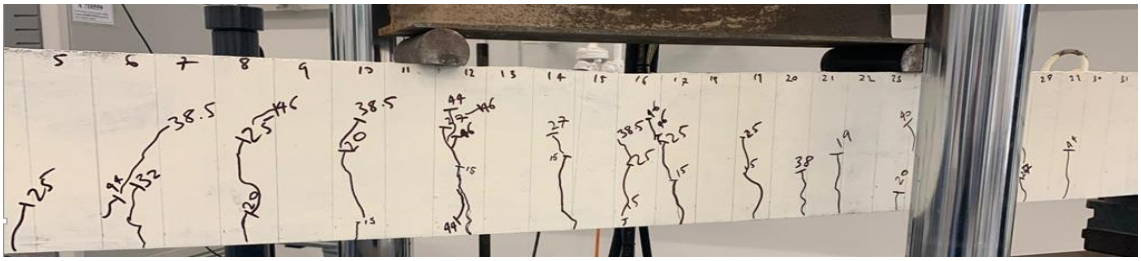

(c)

Figure 8: Development and propagation of crack patterns for carbon steel RC beam CS-D10 at different levels of applied load, including (a) P=15 kN, (b) P=27 kN, (c) $P=P_u$=48.7 kN.

4.4. Deflections

The level of deflection which occurs in structural members during service loading is an important consideration in design, to ensure that the building remains suitable for its intended use and comfortable for occupants. As discussed previously, the stainless steel RC members examined experimentally and discussed in this paper demonstrated significantly greater levels of deflection at failure compared with the carbon steel reinforced concrete beam owing mainly to the inherently ductile properties of stainless steel and its survivability, even at high levels of deflection. In addition, as more cracks developed and the strain concentrations in the cross-section were distributed, this enabled the ductility of the section to be mobilised. In the current section, design approaches for estimating and quantifying acceptable levels of deflection are evaluated.

The level of deflection which is considered ‘acceptable’ is dependent on a number of parameters, including the significance of a given structural member, the type of structure being considered and the applied load (Shamass and Cashell, 2020). The standard approach in typical design codes, including Eurocode 2 (2004) and ACI 318-11 (2011), is to specify an allowable span to overall depth ratio for the concrete element. In Eurocode 2, this limit for carbon steel RC beams, slabs and cantilevers subjected to quasi-permanent loads is span/250, for example. Alternatively, deflections can be obtained and checked against the predefined limits calculated using analytical expressions given in design standards.

In Eurocode 2, the deflection of a member is obtained based on the principle that the member comprises cracked and un-cracked sections. This means that members which are expected to crack, but may not be fully cracked, behave in a manner intermediate between the uncracked and fully cracked conditions.

Consequently, the maximum deflection (δ_{EC2}) for RC members subjected mainly to flexure is determined as:

$$\delta_{EC2} = (1 - \zeta)\delta_1 + \zeta\delta_2 \quad (12)$$

where,

$$\zeta = 1 - \beta\left(\frac{M_{cr}}{M_a}\right)^2 \quad (13)$$

In these expressions, ζ is a distribution coefficient allowing for tension stiffening in the section, β is a coefficient taking account of the influence of the duration of the loading or of repeated loading on the average strain, and $\delta_1$and δ_2 are the maximum deflections for the un-cracked section and cracked section, respectively. The recommended values for ζ and β are zero for the un-cracked portion of the section and unity for single short-term loading, respectively. M_{cr} and M_a represent the bending moment values calculated at the cracking and service loads, respectively. δ_1 and δ_2 are determined from Equations (14 and 15), respectively, for the mid-span values for beams subjected to four point bending conditions:

$$\delta_1 = \frac{Pa}{24E_cI_g}(3L^2 - 4a^2) \quad (14)$$

$$\delta_2 = \frac{Pa}{24E_cI_{cr}}(3L^2 - 4a^2) \quad (15)$$

where L is the clear span, P is each individual applied point load, a is the distance between the support and the nearest loading point, and I_g and I_{cr} are the gross and cracked second moment of areas of the section, respectively. The modulus of elasticity of concrete (E_c) is obtained from Equation (16):

$$E_c = 22000(0.1f_c)^{0.3} \quad (16)$$

and I_g and I_{cr} are calculated based on the principles of elastic analysis using the expressions given in Equations (17 and 18), respectively:

$$I_g = \frac{bh^3}{12} \quad (17)$$

$$I_{cr} = \frac{bd^3k^3}{3} + \mu A_s d^2(1 - k)^2 \quad (18)$$

where $k = \sqrt{2\rho\mu + (\rho\mu)^2} - \rho\mu$

In these expressions, ρ is the reinforcement ratio and μ represents the modular ratio between the reinforcement and the concrete ($\mu = E_s / E_c$).

A similar approach is adopted in ACI 318-11 (2011) for the deflection calculations of a member. However, the ACI 318-11 requires the determination of the effective second moment of area (I_e) based on the second moment of area of the cracked and un-cracked sections, as follows:

$$I_e = \left(\frac{M_{cr}}{M_a}\right)^3 I_g + \left[1 - \left(\frac{M_{cr}}{M_a}\right)^3\right] I_{cr} \quad (19)$$

M_{cr} is calculated using Equation (9), and I_g and I_{cr} are obtained from Equations (17 and 18), respectively. The maximum deflection at the mid-span for beams that are subjected to four point bending conditions is determined as:

$$\delta_{ACI} = \frac{Pa}{24 E_c I_e} (3L^2 - 4a^2) \quad (20)$$

According to the ACI 318-11, the concrete modulus of rupture f_r and the concrete modulus of elasticity E_c are calculated using the expressions given in Equations (11 and 21), respectively.

$$E_c = 4700\sqrt{f_c} \quad (21)$$

In the current analysis, the experimental deflections at two different levels of service load are assessed, namely the deflection value corresponding to 30% and 67% of the ultimate bending moment ($\delta_{0.3}$ and $\delta_{0.67}$), respectively. This approach was also adopted by other researchers (Abed and Alhafiz, (2019; El-Nemr et al., 2013). The results are presented in Table 5 together with the corresponding design values (i.e. $\delta_{EC2,0.3}$, $\delta_{ACI,0.3}$, $\delta_{EC2,0.67}$ and $\delta_{ACI,0.67}$).

With reference to the data presented in Table 5, it is noted that the experimental deflections corresponding to 30% and 67% of M_u (i.e. $\delta_{0.3}$ and $\delta_{0.67,}$ respectively) were significantly greater for the beams reinforced with stainless steel rebars, compared with CS-D10. For the beams reinforced with 10 mm bars, $\delta_{0.3}$ and $\delta_{0.67}$ were 61% and 57% on average higher for SS43-D10 and SS44-D10 compared with the corresponding value from CS-D10. This is expected, owing to the greater levels of strain in the rebar at service loading for beams reinforced with stainless steel bars compared with those with carbon steel reinforcement, and also the greater load-carrying capacity of these members. However, the deflections which develop in RC members prior to failure can be controlled in a number of different ways, depending on the application. For example, different geometries can be selected, and also the deflection criteria may be reviewed for a given application, by employing some engineering judgment.

Further, it is observed that both Eurocode 2 and ACI 318-11 generally provide deflection values which are below the experimental deflection values. At very low load levels (30% of the ultimate bending moment), which is likely to be below service loading in many cases, the deflection estimations from Eurocode 2 ($\delta_{EC2,0.3}$) were found to be greater than the deflections during the tests ($\delta_{0.3}$) in most cases, indicating the conservatism of the code. On the other hand, ACI 318-11 provides deflection values ($\delta_{ACI,0.3}$) lower than the corresponding experimental values in most cases. At greater load levels (67% of the ultimate bending moment), the deflection limits in both design codes ($\delta_{EC2,0.67}$, $\delta_{ACI,0.67}$) were lower than the deflections values obtained from the tests. This un-conservatism was more substantial at the higher load level ($0.67M_u$).

The average values of $\delta_{EC2,0.3}/\delta_{0.3}$ and $\delta_{ACI,0.3}/\delta_{0.3}$ from the tests with 10 mm stainless steel rebars were 1.10 and 1.00, respectively, whilst the corresponding values at $0.67M_u$ were 0.81 and 0.84, respectively. These same values for the equivalent carbon steel RC beam was 1.22 and 1.09 at $0.3M_u$ and 0.91 and 0.95 at $0.67M_u$. This demonstrates that for the carbon steel RC member, CS-D10, both codes generally provide deflection limits which are greater than the deflection which was observed in the test at $0.3M_u$ and slightly lower than that which occurred in the experiment at $0.67M_u$. Similar conclusions were relatively found for stainless steel RC members, SS44-D10 and SS43-D10. However, it is noteworthy that these members had around 10% lower predicted-to-experimental values compared with the corresponding carbon steel member. Hence, the deflection limit as given in the design standards for carbon steel reinforced concrete beams may be considered safe for that application, but are slightly less conservative for stainless steel RC beams, and do not provide a true reflection of the real deflection behaviour. Moreover, given the higher initial cost of stainless steel reinforcement, compared with traditional carbon steel bars, as well as the increasingly important demands to design more efficient and durable structures, it is essential that appropriate design expressions for stainless steel reinforced concrete members are made available. In order to improve the accuracy of deflection predictions for stainless steel RC beams in design codes, it was proposed to employ the secant modulus in the calculations in place of the elastic modulus (Rabi et al., 2021). In this approach, an elastic analysis of the section is conducted to obtain the depth of the neutral axis and the stress in the reinforcement, according to the stress and strain distributions in the section. Since the secant modulus is function of the stress in the reinforcement, an iterative technique is required to obtain the stress in the reinforcement. More detailed descriptions of the procedures are available elsewhere (Rabi et al., 2021). Table 6 presents the deflection limits for stainless steel RC beams obtained using the secant modulus in the deflection calculations in place of the elastic modulus (as is used to determine the values in Table 5). The results show that the predicted deflection values corresponding to service load $0.3M_u$ are very similar regardless of whether the elastic modulus or the secant modulus is employed. However, there is a more notable difference at $0.67M_u$ with the values determined using the secant modulus providing a much

more accurate reflection of the deflection values. For further simplifications to aid practicing engineers, a partial reduction factor for the elastic modulus of stainless steel reinforcement in RC beams is proposed on the basis of the ratio between the secant and elastic moduli. From the results presented in Table 7, the proposed partial reduction factor for the elastic modulus are 1.0 and 0.83 for load levels corresponding to $0.3M_u$ and $0.67M_u$, respectively. It is noteworthy that further parametric study is required to verify the proposed modulus reduction factor using a wide range of geometries and material properties.

Table 5: Analysis of the experimental and design deflection values

Test	Experiment			Eurocode 2				ACI 318-11			
	δ_u (mm)	$\delta_{0.3}$ (mm)	$\delta_{0.67}$ (mm)	$\delta_{EC2,0.3}$ (mm)	$\delta_{EC2,0.3}/\delta_{0.3}$	$\delta_{EC2,0.67}$ (mm)	$\delta_{EC2,0.67}/\delta_{0.67}$	$\delta_{ACI,0.3}$ (mm)	$\delta_{ACI,0.3}/\delta_{0.3}$	$\delta_{ACI,0.67}$ (mm)	$\delta_{ACI,0.67}/\delta_{0.67}$
SS43-D8	21.48	2.11	8.26	3.11	1.47	8.52	1.03	1.98	0.94	8.37	1.01
SS44-D8	20.62	1.67	7.56	2.34	1.40	6.75	0.89	1.44	0.86	6.60	0.87
SS43-D10	23.47	2.69	8.98	3.15	1.17	7.87	0.88	2.78	1.03	8.12	0.90
SS44-D10	25.62	2.93	9.80	2.99	1.02	7.31	0.75	2.84	0.97	7.62	0.78
SS43-D12	24.96	3.53	10.70	3.28	0.93	7.71	0.72	3.36	0.95	8.03	0.75
SS44-D12	23.63	3.40	9.48	2.73	0.80	6.51	0.69	2.78	0.82	6.78	0.72
CS-D10	8.80	1.74	5.97	2.13	1.22	5.45	0.91	1.89	1.09	5.67	0.95
Average for SS					1.13		0.83		0.93		0.84
COV for SS (%)					21.3		14.5		7.7		12.2

Table 6: Analysis of the design deflection values using secant modulus

Test	Eurocode 2				ACI 318-11			
	$\delta_{EC2,0.3}$ (mm)	$\delta_{EC2,0.3}/\delta_{0.3}$	$\delta_{EC2,0.67}$ (mm)	$\delta_{EC2,0.67}/\delta_{0.67}$	$\delta_{ACI,0.3}$ (mm)	$\delta_{ACI,0.3}/\delta_{0.3}$	$\delta_{ACI,0.67}$ (mm)	$\delta_{ACI,0.67}/\delta_{0.67}$
SS43-D8	3.13	1.49	9.90	1.20	1.98	0.94	9.56	1.16
SS44-D8	2.37	1.42	8.51	1.13	1.44	0.86	8.03	1.06
SS43-D10	3.17	1.18	8.68	0.97	2.79	1.04	8.91	0.99
SS44-D10	3.02	1.03	8.57	0.87	2.86	0.97	8.87	0.90
SS43-D12	3.31	0.94	9.12	0.85	3.39	0.96	9.45	0.88
SS44-D12	2.75	0.81	7.50	0.79	2.79	0.82	7.78	0.82
Average for SS		1.14		0.97		0.93		0.97
COV for SS (%)		21.42		15.29		7.63		11.77

Table 7: Proposed partial modulus reduction factor

Test	Eurocode 2			Partial reduction factor	
	E (N/mm^2)	**$E_{sec,0.3}$ (N/mm^2)**	**$E_{sec,0.67}$ (N/mm^2)**	**$E_{sec,0.3}/E$**	**$E_{sec,0.67}/E$**
SS43-D8	156005	154461	130871	0.99	0.84
SS44-D8	178501	175609	135954	0.98	0.76
SS43-D10	148563	147597	131924	0.99	0.89
SS44-D10	179291	177290	147539	0.99	0.82
SS43-D12	186793	184491	151061	0.99	0.81
SS44-D12	198609	196566	165804	0.99	0.83
Average for SS				0.99	0.83

Conclusions

This paper presents a detailed experimental investigation and discussion on the behaviour of stainless steel reinforced concrete beams. The concept of replacing traditional carbon steel rebar with stainless steel reinforcement, to improve the durability, life-span and resilience is not new although there is a distinct lack of performance data available in the existing literature. Moreover, and perhaps as a consequence of the lack of behavioural data, the design guidance available is also very limited and somewhat inappropriate in that it typically does not account for the unique material constitutive response of stainless steel. Accordingly, the motivation for this work was to conduct an experimental programme to investigate the key behavioural aspects, and then also to propose usable design guidance to aid practicing engineers.

The paper describes the results of seven beam tests, six of which comprised stainless steel reinforcement whilst the seventh specimen had carbon steel rebars for comparison. The results and comprehensive performance data which is presented herein, was missing from existing literature. The experimental data is compared with the capacity predictions from a newly-proposed CSM design approach, as well as the guidance in existing international design standards. The key performance measures for reinforced concrete beams are discussed, including the load-deflection response, ultimate capacity, cracking behaviour and deflections at service load. The test results show that RC members reinforced with stainless steel perform very well, and provide an excellent alternative to traditional carbon steel especially for structures exposed to harsh environments. Based on this detailed study and analysis, the following guidance and conclusions are made:

- The results presented in this study show that the ultimate bending moment capacity of stainless steel RC beams was higher than the ultimate moment capacity of an identical beam containing

carbon steel rebars. This is mainly owing to the distinctive mechanical properties of stainless steel reinforcement.

- The other important observation is that using stainless steel bar not only improved the ultimate load capacity of the beams but also enhanced the overall ductility and allowed for much greater deflections to be achieved before failure occurs. A ductile failure mode is very important in structural design especially in applications requiring resilience during extreme events (e.g. an earthquake). However, on the other hand, there may be serviceability issues for stainless steel reinforced concrete beams which require further analysis and investigation.
- The initial load-deflection response of stainless steel RC beams was relatively similar to the carbon steel RC beam. However, later on the response once cracking developed, the stainless steel RC beams exhibited a more nonlinear, rounded, response with a gradual reduction in the load carrying capacity, following attainment of the peak load, thus resulting in a ductile failure.
- The current design standards including Eurocode 2 and ACI 318-11 do not allow for the considerable difference in the constitutive material behaviour of stainless steel and carbon steel. The results presented herein highlight that employing an inappropriate material model in the design of stainless steel RC which does not account for the nonlinear behaviour with significant strain hardening, leads to overly conservative results. Moreover, it does not exploit one of the key advantages of using stainless steel rebar (in addition to the corrosion resistance) which is excellent ductility.
- There was an excellent agreement shown between the experimental capacity values and those obtained analytically using the full and simplified proposed CSM approach with average predicted-to-experimental ultimate moments of 0.91 and 0.88, respectively. Clearly, the full and simplified proposed CSM methods provide less conservative and more appropriate predictions of the ultimate bending moment capacity compared with existing design codes.
- The development of crack patterns were observed to be quite similar for beams reinforced with either stainless steel or carbon steel rebars. However, it was shown that the stainless steel RC beam failed by the crushing of the concrete whereas the carbon steel RC beam failed by yielding of the reinforcement.
- The in-service deflections corresponding to 30% and 67% of the ultimate bending moment of the stainless steel RC beams were greater than those for the carbon steel RC member. This is to be expected, owing to the higher moments that are achieved by the stainless steel RC beams and the greater ductility of the stainless steel rebars. Reinforced concrete members with stainless steel rebars are expected to deflect more than those with traditional carbon steel, because they survive for a much longer period before the rebar ruptures.

- Based on the data examined herein and following detailed analysis on the deflection behaviour of stainless steel RC beams, it is observed that the current procedures for deflection calculations in both EC2 and ACI do not provide accurate reflection of the actual deflections depicted in tests, and therefore new, performance-based analytical equations should be derived for calculating deflections of RC beams with stainless steel. Nevertheless, until proper, verified and reliable analytical equations are made available for RC members with stainless steel reinforcement, it is recommended that the elastic modulus and secant modulus of stainless steel is employed in the deflection calculations at load levels corresponding to $0.3M_u$ and $0.67M_u$, respectively. Alternatively, a more simplified approach may be used by applying a partial modulus reduction factor of 0.83 to the elastic modulus in the deflection calculations at a load level corresponding to $0.67M_u$.

Acknowledgements

The authors would also like to thank the technicians Graham Bird and Paul Elsdon for their continuous support in the Laboratory and acknowledge the Centre for Civil and Building Services Engineering (CCiBSE) at London South Bank University for providing technical supports for this research. In addition, the authors would like to thank Fazal Ur-Rehman for assistance with the stainless steel reinforcement material testing.

Conflict of Interest

The authors wish to confirm that there are no known conflicts of interest associated with this research.

References

Abed, F., & Alhafiz, A.R. (2019). Effect of basalt fibers on the flexural behavior of concrete beams reinforced with BFRP bars. Composite Structures, 215, pp.23-34.

Afshan, S., & Gardner, L. (2013). The continuous strength method for structural stainless steel design. Thin-Walled Structures, 68, pp.42-49.

Alih, S., & Khelil, A. (2012). Behavior of inoxydable steel and their performance as reinforcement bars in concrete beam: Experimental and nonlinear finite element analysis, Construction and Building Materials, 37, pp. 481-492.

Alonso, M.C., Luna, F.J., & Criado, M. (2019). Corrosion behavior of duplex stainless steel reinforcement in ternary binder concrete exposed to natural chloride penetration. Construction and Building Materials, 199, pp.385-395.

Alvarez, S.M., Bautista, A., & Velasco, F. (2011). Corrosion behaviour of corrugated lean duplex stainless steels in simulated concrete pore solutions, Corrosion Science, 53(5), pp. 1748-1755.

American Concrete Institute (ACI), (2011). Building code requirements for structural concrete (ACI 318-11) and commentary. ACI 318R-11, Farmington Hills, MI.

Baddoo, N.R. (2008). Stainless steel in construction: A review of research, applications, challenges and opportunities, Journal of Constructional Steel Research, 64(11), pp. 1199-1206.

Baddoo, R. & Burgan, A. (2012). Structural Design of Stainless Steel, SCI Publication No. P291. The Steel Construction Institute.

British Stainless Steel Association. (2003). The use of stainless steel reinforcement on bridges'. Available at: http://www.bssa.org.uk/cms/File/REBar%20report.pdf (Accessed: 11 April 2017).

BS 4449+A3. (2005): Steel for the reinforcement of concrete. Weldable reinforcing steel. Bar, coil and decoiled product. Specifications', British Standards Institution.

BS 6744. (2016). Stainless steel bars for the reinforcement of concrete. Requirements and test methods', British Standards Institution.

Calderon-Uriszar-Aldaca, I., Briz, E., Larrinaga, P., & Garcia, H. (2018). Bonding strength of stainless steel rebars in concretes exposed to marine environments, Construction and Building Materials, 172, pp. 125-133.

Cramer, S., Covino, B., Bullard, S., Holcomb, G., Russell, J., Nelson, F., Laylor, H., & Soltesz, S. (2002). Corrosion prevention and remediation strategies for reinforced concrete coastal bridges, Cement and Concrete Composites, 24(1), pp. 101-117.

El-Nemr, A., Ahmed, E.A., & Benmokrane, B., (2013). Flexural Behavior and Serviceability of Normal-and High-Strength Concrete Beams Reinforced with Glass Fiber-Reinforced Polymer Bars. ACI structural journal, 110(6).

EN 10088-1. (1995). Stainless steels. List of stainless steels, British Standards Institute.

EN 12390-3. (2009). Testing hardened concrete Part 3: Compressive strength of test specimens, European Committee for Standardization (CEN).

EN 1992-1-1. (2004). Eurocode 2: Design of concrete structures part 1-1: General rules and rules for buildings', European Committee for Standardization (CEN).

EN 6892-1. (2016). Metallic materials- Tensile testing part 1: Method of test at room temperature, European Committee for Standardization (CEN).

Evans, K. (2002). RB Rebak in Corrosion Science–A Retrospective and Current Status in Honor of Robert P, Frankenthal, PV, 13, pp. 344-354.

Fahim, A., Dean, A.E., Thomas, M.D., & Moffatt, E.G., (2019). Corrosion resistance of chromium-steel and stainless steel reinforcement in concrete. Materials and Corrosion, 70(2), pp.328-344.

Gardne, L., Bu, Y., Francis, P., Baddoo, NR., Cashell, KA., & McCann, F. (2016). Elevated temperature material properties of stainless steel reinforcing bar. Constr Build Mater; 114:977–97.

Gardner L., & Nethercot D.A. (2004). Structural stainless steel design: a new approach. Journal of Structural Engineering, 82(21),pp. 21-30.

Gardner, L. (2005). The use of stainless steel in structures, Progress in Structural Engineering and Materials, 7(2), pp. 45-55.

Gardner, L., Wang, F., & Liew, A. (2011). Influence of strain hardening on the behavior and design of steel structures, International Journal of Structural Stability and Dynamics, 11(05), pp. 855-875.

Gardner, L., Yun, X., Macorini, L., & Kucukler, M. (2017). Hot-rolled steel and steel-concrete composite design incorporating strain hardening, Structures, 9, pp. 21-28.

Gedge, G. (2003). Rationale for using stainless steel reinforcement in the UK construction industry, Arup Materials Consulting, UK.

Li, Q., Guo, W., Liu, C., Kuang, Y., & Geng, H., (2020). Experimental and Theoretical Studies on Flexural Performance of Stainless Steel Reinforced Concrete Beams. Advances in Civil Engineering, 2020.

Lollini, F., Gastaldi, M., & Bertolini, L., (2018). Performance parameters for the durability design of reinforced concrete structures with stainless steel reinforcement. Structure and Infrastructure Engineering, 14(7), pp.833-842.

Medina, E., Medina, J.M., Cobo, A., & Bastidas, D.M. (2015). Evaluation of mechanical and structural behavior of austenitic and duplex stainless steel reinforcements, Construction and Building Materials, 78, pp. 1-7.

Mirambell, E., & Real, E. (2000). On the calculation of deflections in structural stainless steel beams: an experimental and numerical investigation, Journal of Constructional Steel Research, 54(1), pp. 109-133.

NA to BS EN 1992-1-1-2004. (2009). UK National Annex to Eurocode 2: Design of concrete structures - Part 1-1: General rules and rules for buildings', British Standards Institution (BSI).

Rabi, M., Cashell, K., & Shamass, R. (2019a). Flexural analysis and design of stainless steel reinforced concrete beams, Engineering Structures, 198, pp. 109432.

Rabi, M., Cashell, K.A., & Shamass, R. (2019b). Analysis of concrete beams reinforced with stainless steel, Proceedings of the fib Symposium 2019: Concrete-Innovations in Materials, Design and Structures, pp. 690-697.

Rabi, M., Cashell, K., & Shamass, R. (2021). Ultimate behaviour and serviceability analysis of stainless steel reinforced concrete beams. Engineering Structures, 248, p.113259.

Rabi, M., Cashell, K.A., Shamass, R., & Desnerck, P., (2020). Bond behaviour of austenitic stainless steel reinforced concrete. Engineering Structures, 221, p.111027.

Rabi, M., Shamass, R. and Cashell, K.A., (2022). Structural performance of stainless steel reinforced concrete members: A review. Construction and Building Materials, 325, p.126673.

Ramberg, W., & Osgood, W.R. (1943). Description of stress-strain curves by three parameters, Issue 902 of National Advisory Committee for Aeronautics Technical Note.

Rasmussen, K.J.R. (2003). Full-range stress–strain curves for stainless steel alloys, Journal of Constructional Steel Research, 59(1), pp. 47-61.

Serdar, M., Žulj, L.V., & Bjegović, D. (2013). Long-term corrosion behaviour of stainless reinforcing steel in mortar exposed to chloride environment, Corrosion Science, 69, pp. 149-157.

Shamass, R., & Cashell, K.A., (2018). Analysis of Stainless Steel-Concrete Composite Beams, Journal of Constructional Steel Research, 152, pp. 132-142.

Shamass, R., & Cashell, K.A., (2020). Experimental investigation into the flexural behaviour of basalt FRP reinforced concrete members. Engineering Structures, 220, p.110950.

Val, D.V., & Stewart, M.G., (2003). Life-cycle cost analysis of reinforced concrete structures in marine environments, Structural safety, 25(4), pp.343-362.

Zhou, Y., Ou, Y., & Lee, G.C. (2017). Bond-slip responses of stainless reinforcing bars in grouted ducts', Engineering Structures, 141, pp. 651-665.